Charge-Collection Characteristics of Low-Power Ultrahigh Speed, Metamorphic AlSb/InAs High-Electron Mobility Transistors (HEMTs)

Dale McMorrow, J. Brad Boos, Alvin R. Knudson, Stephen Buchner, Ming-Jey Yang, Brian R. Bennett, and Joseph S. Melinger

Abstract—**Time-resolved charge-collection measurements are performed on AlSb/InAs HEMTs with pulsed laser excitation as a function of device bias conditions and the incident laser pulse energy. The results provide clear evidence for the presence of charge-enhancement processes that, in many ways, are analogous to those observed previously for GaAs FET technology.**

I. Introduction

LOW-VOLTAGE low-power-consumption electronics will be critical in future high-speed analog and digital applications that require lightweight power supplies, long battery lifetimes, improved efficiency, or high component density. Low-noise applications which would significantly benefit from reduced power consumption include transmit/receive modules for space-based communications, mm-wave imaging arrays, remote earth sensing arrays, portable communications, and micro-air vehicles. Digital circuits operating at speeds approaching 100 GHz with low power consumption are required for applications in multi-function radar and communication systems. The high current drive capability and potentially low power-delay product make the AlSb/InAs HEMTs attractive candidates for high-speed logic applications, particularly when combined with Sb-based resonant interband tunneling diodes for enhanced functionality and low drain voltage operation [1].

In this paper we present the first investigation into the single-event-effects (SEE) performance of the AlSb/InAs HEMT technology. This new high-speed, low-power (0.5 V) technology represents a low-cost alternative to InP-based HEMTs, with the potential for surpassing the performance of InP HEMT technology (InP-based HEMTs currently hold the record in current gain cutoff frequency for any three-terminal semiconductor device [2]–[4]). The laser-induced charge-collection measurements presented here represent the first look into the potential utility of this technology for use in the radiation environment of space. The results reveal characteristics that are analogous in many ways to those of GaAs field-effect transistor (FET) technologies [5], [6], and suggest that SEE mitigation methodologies similar to those used for GaAs FETs may be appropriate.

Manuscript received July 25, 2000. This work was supported by the Office of Naval Research

D. McMorrow and J. S. Melinger are with the Naval Research Laboratory, Code 6823, Washington, DC 20375 USA.

J. B. Boos is with the Naval Research Laboratory, Code 6856, Washington, DC 20375 USA.

M.-J. Yang and B. R. Bennett are with the Naval Research Laboratory, Code 6876, Washington, DC 20375 USA.

A. R. Knudson and S. Buchner are with SFA, Inc., Largo, MD USA (under contract to NRL).

Publisher Item Identifier S 0018-9499(00)11165-7.

II. InAs HEMT Technology

The material properties that have the greatest impact on increasing the speed and decreasing the operating voltage in HEMTs are the sheet charge density in the 2-DEG and the effective electron velocity in the channel. In recent years this has led to the increased use of $In_xGa_{1-x}As$ channel HEMTs with higher and higher mole fractions of In. Increasing the In concentration results in higher electron mobility and velocity in the channel and a larger conduction-band offset which leads to a higher sheet charge density. $In_xGa_{1-x}As$ channel HEMTs with an In content of over 50% are typically grown on an InP substrate rather than a GaAs substrate due to the better lattice match with InP. Compared to GaAs-based HEMTs, InP-based HEMTs have clear performance advantages. However, InP-based pseudomorphic HEMT channel designs with substantially higher In content than the $In_{0.53}Ga_{0.47}As$ lattice-matched composition have increased restrictions on layer thickness due to lattice mismatch. Therefore, the improvement in the channel transport properties of these devices has been limited by deleterious lattice strain effects and interface scattering.

An attractive low cost alternative to InP-based HEMTs is the growth of high In content channel HEMTs on GaAs substrates, commonly referred to as metamorphic HEMTs. This approach is becoming increasingly popular due to the use of the less brittle, larger diameter (6 inch) GaAs substrates to increase throughput and yield, and because it offers the ability to optimize the In content in the channel for the particular power, low noise, or logic application desired. State-of-the-art millimeter-wave power densities and low noise amplifier performance recently have been achieved using this approach [7], [8].

The 6.1 Å material system, consisting of InAs, GaSb, AlSb, and related alloys, offers the potential of metamorphic HEMT circuits operating at lower power and higher speed than InP-based circuits. AlSb/InAs HEMTs that have only InAs as the channel material have the potential to set a new standard for speed and power consumption due to the high mobility, velocity, and sheet charge density that can be achieved in this material system [9]. The combination of high peak electron velocity

0018–9499/00$10.00 © 2000 IEEE

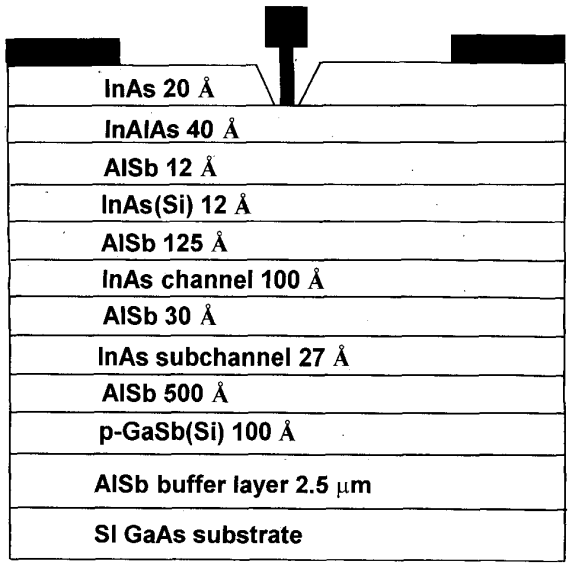

Fig. 1. Schematic diagram illustrating the AlSb/InAs HEMT device structure.

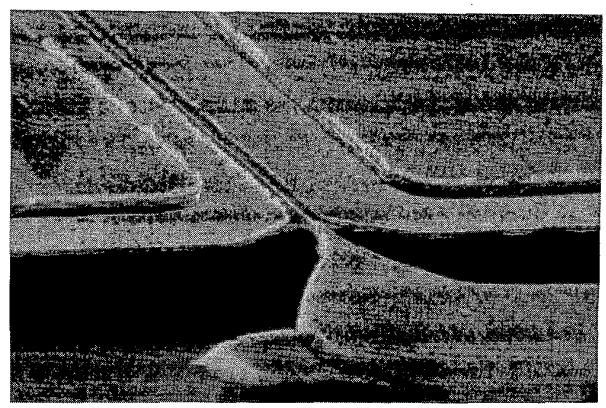

Fig. 2. SEM micrograph of gate air bridge at mesa edge. $L_G = 60$ nm, $L_{DS} = 1.0$ μm.

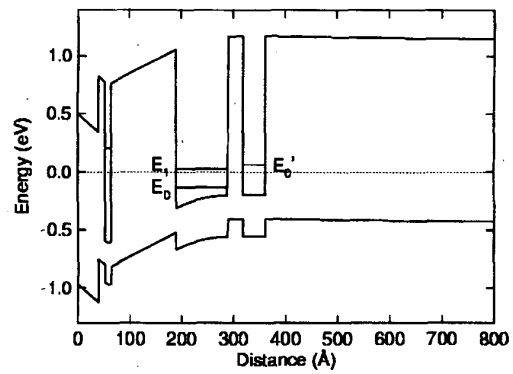

Fig. 3. Calculated band structure for InAs HEMT device structure of Fig. 1 (from ref. [11]).

(4×10^7 cm/sec) at low electric field and high channel conductivity enable operation at very low drain voltages. Metamorphic HEMTs with InAs channels and AlSb barriers operating at a drain voltage of only 100 mV exhibit measured unity-current-gain cutoff frequencies (f_T) of 90 GHz, the highest reported for any field-effect transistor at this low voltage [10]. At $V_{DS} = 0.5$ V, the measured f_T of a 0.1 μm gate HEMT was 250 GHz (after bonding pad capacitance had been subtracted) [11].

III. Experimental

The laser-induced charge collection measurements are performed with nominally 1 ps duration optical pulses centered at 590 nm (2.1 eV) at a pulse repetition rate of 12 kHz. All experiments were performed at room temperature (295K). The optical pulses are focused onto the device under test (DUT) with a 100× microscope objective, resulting in a measured Gaussian spot size of 1.2 μm at the surface of the DUT [12]. The DUT is mounted on a motorized xyz stage with 0.1 μm resolution. For all of the experiments reported here, the laser spot is focused between the gate and drain of the transistor, with the spot position and focus optimized to produce the largest amplitude signals. The pulse energy is monitored with a calibrated large-area photodiode. The incident pulse energy is converted into deposited charge by correcting for reflection losses and assuming that each photon gives rise to a single electron-hole pair.

The DUT is mounted in a high-frequency (50 GHz) microwave package with the gate and drain wire-bonded to microstrip transmission lines and the source grounded. The transient signals are launched from the microstrip lines into a piece of 50 GHz coaxial cable, passed through a 50 GHz bias tee, and into the input of a 20 GHz sampling oscilloscope [5].

The AlSb/InAs HEMT material was grown by molecular beam epitaxy on a semi-insulating (100) GaAs substrate. A cross section of the layer design is shown in Fig. 1, with a scanning-electron micrograph of a 60 nm gate length device illustrating the surface morphology and the gate metal air bridge shown in Fig. 2. A 2.5 μm undoped AlSb buffer layer is used to accommodate the 7% lattice mismatch between the GaAs substrate and the HEMT layer structure.

The band diagram corresponding to the HEMT device structure of Fig. 1, illustrating the InAs channel and sub-channel, is shown in Fig. 3. The sub-channel is included to reduce impact ionization effects in the channel [11]. The band structure of Fig. 3 was calculated using a finite-difference model for the one-dimensional Poisson equation [9]. The effects of the two-dimensional density of states and spatial redistribution of confined carriers were calculated using the Schroedinger equation for the quantum well region. Strain effects were not included in this calculation. Additional characteristics of the design and fabrication are described elsewhere [9]–[11].

In this study we report results for 0.1 μm gate length depletion-mode HEMTs with source-drain spacings of 2, 3, and 4 μm. A typical set of drain characteristics for HEMTs with a 0.1 μm gate length and a 4 μm source-drain spacing is shown in Fig. 4. At $V_{DS} = 0.4$ V, a transconductance above 400 mS/mm is observed. The S-parameters of the HEMTs were measured on-wafer from 1 to 40 GHz. For devices with a 1 μm source-drain spacing maximum f_T and $f_{\max}$ values of 130 GHz and 60 GHz are measured, respectively. When external parasitic effects are removed, an f_T of 200 GHz is obtained.

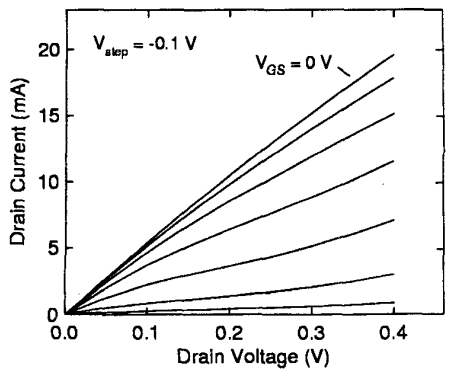

Fig. 4. Drain characteristics of HEMT device used in this study: $L_G = 0.1$ μm, $W_G = 100$ μm, $L_{DS} = 4.0$ μm, $V_{GS} = -0.1$ V/step.

The results of this study are impacted by the optical properties of the constituent materials. InAs and GaSb are direct-gap semiconductors with bandgaps of 0.35 and 0.67 eV, respectively. The absorption coefficients for these materials at 590 nm (2.1 eV) are 1.52×10^5 cm^{-1} and 3.84×10^5 cm^{-1}, respectively [13], [14]. These compare to a value gap at 1.6 eV with an absorption coefficient at 2.1 eV of 1.3×10^3 cm^{-1} [15], [16]. This is a factor of 40 less than that of GaAs, and corresponds to a 1/e optical penetration depth of 7.7 μm of 5.1×10^4 cm^{-1} for GaAs. AlSb, in contrast, has an indirect.

IV. Results and Discussion

Gate and drain charge-collection transients have been measured for pulsed laser excitation as a function of a range of parameters, including gate and drain bias conditions, laser pulse energy, and the laser spot position.

A. Gate Bias Dependence

Fig. 5 shows a series of drain charge-collection transients measured as a function of gate bias. The data exhibit a strong dependence on gate bias, with the transients changing significantly in both shape and amplitude as the gate bias is varied. These data illustrate clearly the presence of long-lived (several ns) contributions to the charge-collection process that become more prevalent as the gate is biased more positive. In contrast, when the device is strongly pinched off ($V_{GS} = -0.70$ V), the long-lived contributions are suppressed.

The results of Fig. 5 are reminiscent of data reported previously for GaAs MESFETs and HFETs [5], [6]. Experiments and computer simulation studies on GaAs FETs have determined that the "direct" collection of deposited charge is quite rapid, typically complete within the first few hundred picoseconds, and that any additional persistent signal contributions are a consequence of source-drain current pathways that are switched on by the perturbing effects of the ionizing radiation [6]. The data of Fig. 5 suggest that similar charge-enhancement processes are involved in the charge-collection dynamics of InAs HEMTs.

The data of Fig. 5 illustrate the presence of processes that occur on two distinct timescales. Following the initial rise, the signal decays initially on a time scale of a few hundred picoseconds. At longer times there exists a persistent background signal

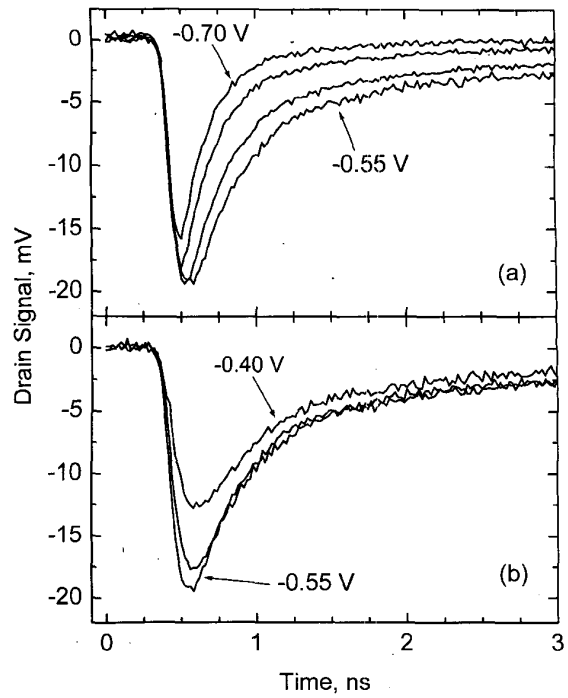

Fig. 5. Drain charge-collection transients measured as a function of gate bias for a device with a 2 μm S-D spacing. $V_{DS} = 0.25$ V; deposited charge, Q_D, is 305 fC. (a) Top to bottom, $V_G = -0.70$ V, -0.65 V, -0.60 V, and -0.55 V; (b) the middle curve is for $V_{GS} = -0.50$ V, and note that the $V_{GS} = -0.55$ V curve is shown in each panel for reference.

that decays on a timescale of a few nanoseconds. This temporal signature is similar to that observed previously for GaAs FETs for which the faster decaying contribution has been assigned [6], [17] to charge collection from a bipolar-like gain process in which the ionizing event leads to a reduction of the source/substrate barrier, with the resultant injected electrons propagating through the substrate to the drain. This source-substrate-drain current pathway typically is significant on the time scale of one to a few hundred picoseconds and, in GaAs, depends sensitively on the injected carrier density [17]. In the present case, the "substrate" would be the 2.5 μm thick AlSb layer.

For GaAs FETs the slower relaxation has been identified through computer simulation [6], [18] as arising from a channel-modulation effect in which excess holes that accumulate under the active region of the device serve to backgate the channel. This current pathway persists as long as the excess hole density is present.

It is noteworthy that the transients of Fig. 5 are significantly slower (broader) and exhibit less detailed structure than those previously measured for GaAs MESFETs [6]. The broadening, which is illustrated by the data of Fig. 6, has contributions from both components of the HEMT transient. Both the rise and decay of the faster component are slower than that of the GaAs MESFET. Also, the slower, nanosecond timescale contribution exhibits a larger amplitude and slower decay time than is typically observed for GaAs FETs. Assuming that the backgating (channel modulation) mechanism is responsible for this latter signal component, then it may be concluded that

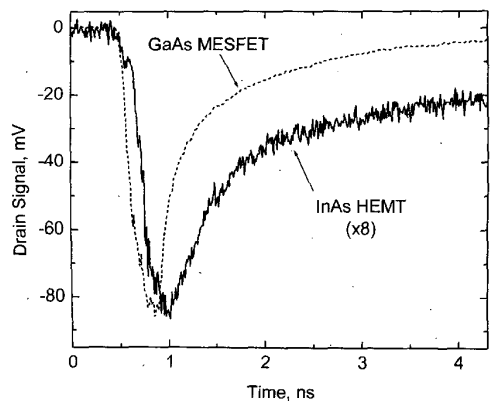

Fig. 6. Drain charge-collection transient for a 4 μm S-D spacing InAs HEMT compared to that for a GaAs MESFET. Deposited charge is 466 fC for each device. The InAs HEMT transient is scaled by a factor of 8. Both devices are biased somewhat "on" with $V_{DS} = 0.25$ V and $V_{GS} = -0.55$ V for the HEMT, and $V_{DS} = 2.5$ V; $V_{GS} = -0.21$ V for the MESFET.

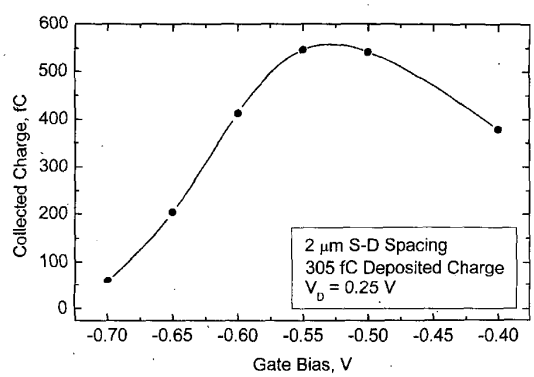

Fig. 7. Integrated drain charge-collection for the data of Fig. 5. The line is included to guide the eye. $V_{DS} = 0.25$ V.

the excess holes have a longer lifetime in the InAs device. This conclusion is consistent with the band diagram of Fig. 3, which indicates that holes generated in the InAs channel and subchannel will migrate to the AlSb barrier layers. The physical separation of the electrons (in the InAs channel) and holes (in the AlSb barriers) will inhibit recombination.

Also evident in the data of Fig. 5 is a "rolling over" of the current pulse amplitude that occurs when the device is biased strongly "on" (as the gate bias is made more positive after the peak amplitude has been achieved). This roll-over is accompanied by additional broadening, and has not been reported previously for GaAs devices (largely due to limitations of previously used experimental setups), but is fully expected. The roll-over occurs when the DC source-drain current becomes large.

This roll-over effect is illustrated clearly in the data of Fig. 7, which show the time-integrated charge-collection behavior as a function of gate bias for the data of Fig. 5. To obtain these results, the individual data curves were integrated to 10 ns (not shown). The data of Fig. 7 reveal three key points. First, they reveal clearly the roll-over in the charge-collection efficiency as the device is biased more strongly on, as is discussed above. Second, they reflect the results of Fig. 5 in illustrating the increase in the charge-collection efficiency as the gate is biased more "on" from pinch off, behavior that is indicative of the presence of charge-enhancement processes. And, finally, the data of Fig. 7 show that the InAs HEMTs of this study experience a net ionization-induced gain (net charge enhancement) under certain bias conditions.

For the range of parameters investigated in Figs. 5 and 7 the maximum charge-collection efficiency (CCE[1]) observed for the InAs HEMT is 1.8. This number is significantly lower than that measured previously[2] for GaAs FETs, with CCEs as high as 60 having been reported [5]. To verify the validity of this conclusion, the CCE of a GaAs MESFET was measured in the present apparatus under equivalent experimental conditions. Representative transients are shown in Fig. 6. Consistent with previous measurements, we observe significant charge enhancement for the MESFET[3] (the CCE is a factor of 4 larger than that of the InAs HEMT). Also, the shape of the transients of the two device types exhibits distinct differences. As noted above, the MESFET transient is narrower with faster. We note that the results of Figs. 5 and 7 are for the 2 μm source-drain (S-D) spacing device. For a given set of experimental conditions, the CCE is typically less for the devices with 3 μm and 4 μm S-D spacings (*vide infra*).

B. Gate Current Transients

One notable characteristic of the InAs HEMT charge-collection data is the apparent lack of any prompt, instrument-limited component, as is commonly observed for the case of GaAs FET technology [6]. In GaAs devices, for 600 nm optical excitation, this prompt feature typically exhibits an amplitude that is comparable to that of the slower contributions, with the dynamics given by a mirror image (about $V = 0$) of the charge collection signal measured at the gate electrode (as is required by charge conservation arguments and is illustrated in [19]). To address this issue, Fig. 8 shows gate and drain current transients measured under identical conditions of bias and laser pulse energy. The gate transient of Fig. 8 is plotted on an expanded scale in Fig. 9.

The amplitude of the gate transient is a factor of 6 smaller than that of the drain transient in this example, with a factor of 25 observed for lower pulse energy excitation.[4] Careful inspection of the leading edge of the drain transient, however, reveals a slight shoulder with an amplitude of approximately 8 mV, equivalent to that of the gate transient. This shoulder is a consequence of hole collection at the gate. The data of Fig. 8, therefore, reveal that gate charge collection is reduced significantly when compared to the analogous GaAs devices (for analogous excitation conditions) and, further, indicate that the drain transients measured for the InAs HEMT are composed largely

[1]CCE is the ratio of the collected change to that deposited by the ion or laser pulse.

[2]It should be noted that all previous charge collection measurements on GaAs FETS have been proformed in tha upward sloping portion of the curve, well below maximum efficiency point.

[3]Agian, this measurenent was not proformed at the peak of the charge collection curve; the value quoted should be treated as illustrative only.

[4]In this example, the pulse energy was increased to obtain a reasonable S/N for the gate transient, at the cost of significant saturation of the drain charge collection amplitude.

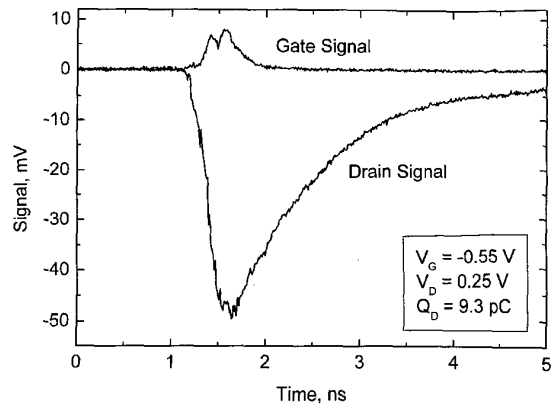

Fig. 8. Gate and drain charge-collection transients measured under identical conditions. $V_{DS} = 0.25$ V; $V_{GS} = -0.55$ V; 9.3 pC deposited charge.

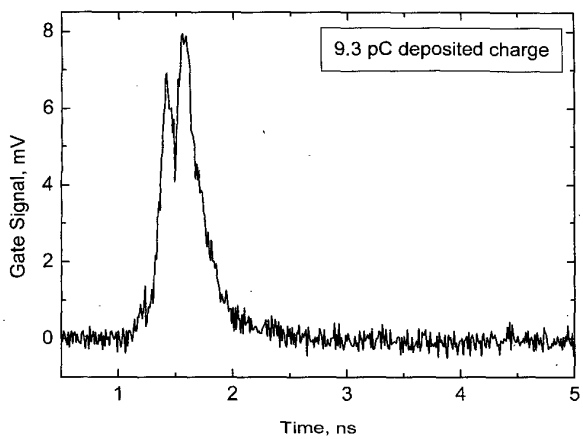

Fig. 9. Gate charge-collection transient of Fig. 8 shown on expanded scale. $V_{DS} = 0.25$ V; $V_{GS} = -0.55$ V.

of the source-drain currents associated with enhancement processes, analogous to the case of GaAs FETs.

C. Pulse Energy Dependence

Charge collection transients have been measured for each of the devices of this study as a function of the incident pulse energy under a variety of bias conditions. Representative data for a 2 μm S-D spacing device is shown in Fig. 10 for two different bias conditions, with the time-integrated representation of this data plotted in Fig. 11. These data illustrate clearly the narrowing of the transient as the gate bias is made more negative, in accordance with the results of Fig. 5. Also evident is the monotonic increase in amplitude (and integrated charge) with increasing pulse energy. The sub-linear dependence of the collected charge on incident pulse energy is indicative of a saturation effect, the precise origin of which is not clear at the present time.

The most striking aspect of the data of Fig. 10 is the surprising lack of dependence of the shape of the transient on the incident pulse energy. Comparison of the normalized lowest (61 fC) and highest (914 fC) energy transients at each bias point reveals very

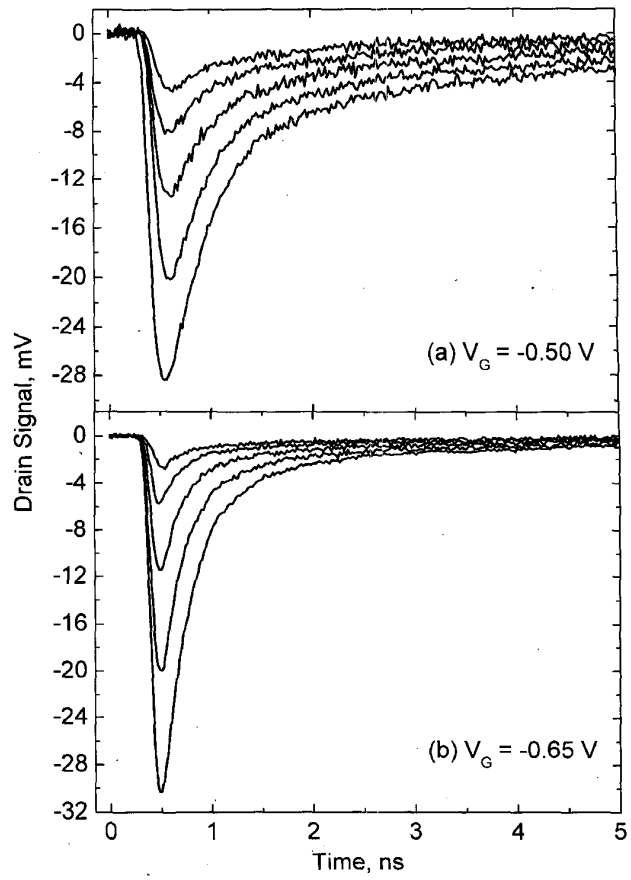

Fig. 10. Drain charge-collection transients measured as a function of laser pulse energy (plotted as deposited charge) for two different gate biases. From bottom (largest amplitude) to top (smallest amplitude): 914 fC, 457 fC, 228 fC, 114 fC, 61 fC; $V_{DS} = 0.25$ V; $D_{SD} = 2$ μm.

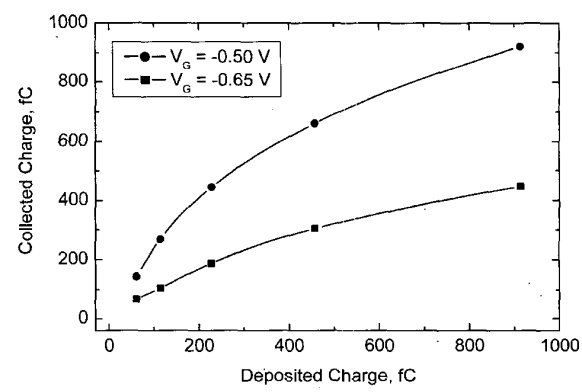

Fig. 11. Time-integrated drain charge-collection for the data of Fig. 10. $V_{DS} = 0.25$ V; $D_{SD} = 2$ μm.

little difference in shape. This result is in stark contrast to the behavior of GaAs FETs, for which the shape of the transient undergoes significant evolution as a function of pulse energy [5], [17], [19]. In GaAs devices the integrated charge is highly sensitive to the injected carrier density, exhibiting a quadratic dependence at low pulse energies, becoming linear at intermediate energies,

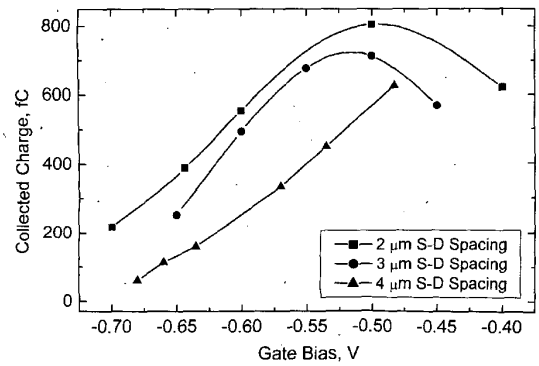

Fig. 12. Time-integrated drain charge-collection as a function of gate bias for three different devices. $V_{DS} = 0.25$ V; $Q_D = 435$ fC.

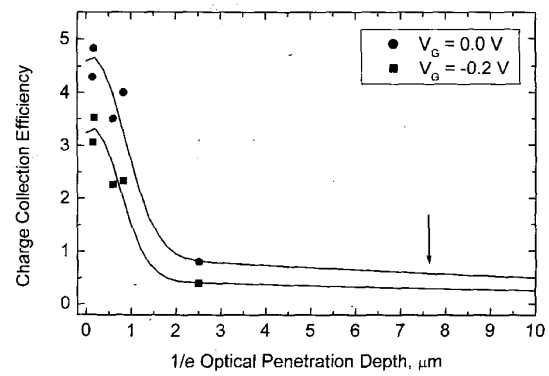

Fig. 13. Charge-collection of a GaAs MESFET plotted as a function of the optical penetration depth of the incident laser pulse. $Q_D = 150$ fC.

and eventually saturating at the higher pulse energies [12]. This behavior is largely due to changes in the amplitude and shape of the 100 ps time-scale contribution (which is identified with a bipolar-like gain process) with changes in the injected carrier density. The absence of analogous behavior in the InAs devices may be a consequence of differences in the material properties of the two devices, in particular those of the AlSb buffer layer.

D. Dependence on Source-Drain Spacing

Measurements performed as a function of source-drain spacing can provide insight into charge-collection mechanisms, particularly the role of parasitic bipolar gain effects [20]. Because processing variations can shift device characteristics (such as the pinch-off voltage), it is difficult to compare directly the charge collection measurements performed on different devices, even if identical bias conditions are used. To circumvent this issue, in Fig. 12 we plot the integrated collected charge for devices with 2 μm, 3 μm, and 4 μm source-drain spacings as a function of gate bias under identical conditions of drain bias and the incident pulse energy. These data reveal that, for all bias points, the charge collection efficiency increases as the source-drain spacing is decreased. This trend is in accordance with that expected if a parasitic bipolar effect plays a significant role in the charge collection process. This result, therefore, supports the assertion that, analogous to the case of GaAs FETs, the rapidly decaying (on the order of a few hundred picoseconds) signal contribution is associated with a bipolar-like charge-enhancement process.

E. Discussion

Since the charge-enhancement processes of GaAs FETs are mediated largely by carriers deposited in the top 2 μm of the device [6], [17], it is necessary to address the possible role of the AlSb buffer layer in shaping the charge collection dynamics. As is noted above, AlSb is an indirect-gap semiconductor material which, at 590 nm (2.1 eV), has a 1/e optical penetration depth of 7.7 μm. This is in contrast to the 0.18 μm penetration depth of GaAs at the same wavelength. Therefore, for equivalent incident pulse energies, the carrier density produced in AlSb will be approximately 2 orders-of-magnitude lower than that of GaAs.

A previous study of GaAs MESFET charge collection on the optical penetration depth provides insight into this phenomena [12]. Using data presented in [12], Fig. 13 shows the variation of the charge collection efficiency of a GaAs FET on the optical penetration depth. As is evident, the charge collection efficiency falls off dramatically for charge deposition below approximately 1.5 μm. Assuming that the charge-enhancement processes of the InAs devices have similar physical origins, qualitatively similar behavior is expected. The arrow in Fig. 13 highlights the 7.7 μm optical penetration depth characteristic of AlSb at 590 nm. It is clear from these data that, for analogous excitation conditions in GaAs (e.g., 7.7 μm penetration depth), the charge enhancement processes are inefficient. Therefore, it is expected that the direct deposition of carriers into the AlSb buffer layer will be a minor contributor to the charge collection and enhancement processes in InAs HEMTs.

In contrast to the AlSb buffer, the InAs channel and sub-channel have a very high absorption coefficient (1.52×10^5 cm^{-1}), with a 1/e optical penetration depth of 0.07 μm at 590 nm. Thus, for 590 nm excitation, approximately 16% of the pulse energy is deposited in the channel and subchannel. For an excitation pulse capable of depositing 500 fC of charge, this corresponds to an initial carrier density on the order of 8.5×10^{18} e-h/cm^3. In contrast, the carrier concentration near the top of the AlSb buffer layer would be 4×10^{16} e-h/cm^3, more than two orders-of-magnitude lower than in the channel.

Therefore, the charge deposition profile in these devices following optical excitation is quite complex, as is the carrier evolution following excitation. It is expected that electrons deposited into the channel will remain constrained within the deep wells of the channel. The holes, however, are expected to migrate to the 125 Å AlSb layer near the surface of the device (immediately above the channel; *cf.*, Fig. 3). It is likely that the excess hole concentration in the AlSb layer contributes to both the bipolar-like response that is evident in the charge collection transient data, and also the several-nanosecond timescale response that is attributed to a channel-modulation (backgating) mechanism.

These measurements reveal clearly, however, that charge-enhancement processes are initiated by the laser pulse, and that

charge injection from the source in a bipolar-like gain process is likely. Analogous (but not identical) behavior is expected for heavy-ion excitation. The lower charge-collection efficiencies measured in the present optical experiments, when compared to those of GaAs FETs, appear to be related, at least in part, to the lower absorption coefficient of the AlSb material (and the corresponding lower carrier densities in the upper regions of the device). Understanding the finer details associated with the charge collection and enhancement processes in these devices will require additional experiments and detailed computer simulations.

V. Conclusions

The charge-collection measurements presented here represent the first view into the SEE response of an exciting new high-performance technology. The pulsed laser results provide clear evidence for the presence of charge-enhancement processes in AlSb/InAs HEMTs, and suggest that the mechanisms are similar to those described previously for GaAs devices.

The shape of the charge-collection transients and the dependence of the charge-collection efficiency on gate bias suggests the presence of bipolar-like and channel-modulation processes that give rise to enhanced source-drain current. The dependence of the charge-collection efficiency on the source-drain spacing provides further support for a bipolar-like gain process.

Conversely, the lack of dependence of the shape of the charge-collection waveform on the deposited charge density deviates from the behavior observed for GaAs FETs, complicating interpretation of the data. Changes in the shape of the transients with the injected carrier density are a particularly clear indicator of bipolar-like gain in GaAs FETs. The present measurements suggest that the devices are in the saturation region of the collected charge vs. deposited charge curve, for which little change in shape is expected. The origin of this behavior is not entirely clear at the present time, but may be associated with an efficient and persistent accumulation of holes in the upper layers of the device.

The very complex nature of the devices of this study, and the variations in material properties within the device, make a precise description of the charge collection processes difficult. Additional experiments and computer simulation studies will be required to address the issues introduced by this study.

References

[1] B. R. Bennett, A. S. Bracker, R. Magno, J. B. Boos, R. Bass, and D. Park, "Monolithic integration of resonant interband tunneling diodes and high electron mobility transistors in the InAs/GaSb/AlSb material system," *J. Vac. Sci. Technol. B*, vol. 18, p. 1650, 2000.

[2] K. H. G. Duh, P. C. Chao, S. M. J. Liu, P. Ho, M. Y. Kao, and J. M. Ballingall, "A super low-noise 0.1 μm T-gate InAlAs/InGaAs/InP HEMT," *IEEE Microwave Guided Wave Lett.*, vol. 1, p. 114, 1991.

[3] P. M. Smith, S. J. Liu, M. Y. Kao, P. Ho, S. C. Wang, K. H. G. Duh, S. T. Fu, and P. C. Chao, "W-band high-efficiency InP-based power HEMT with 600 GHz $f_{\max}$," *IEEE Microwave Guided Wave Lett.*, vol. 5, p. 230, 1995.

[4] L. D. Nguyen, A. S. Brown, M. A. Thompson, and L. M. Jelloian, "50-nm self-aligned-gate pseudomorphic AlInAs/GaInAs high-electron mobility transistors," *IEEE Trans. Electron Dev.*, vol. 39, p. 2007, 1992.

[5] D. McMorrow, J. S. Melinger, N. Thantu, A. B. Campbell, T. R. Weatherford, A. R. Knudson, L. H. Tran, and A. Peczalski, "Charge collection mechanisms of heterostructure FETs," *IEEE Trans. Nucl. Sci.*, vol. 41, p. 2055, 1994.

[6] D. McMorrow, T. R. Weatherford, S. Buchner, A. R. Knudson, J. S. Melinger, L. H. Tran, and A. B. Campbell, "Single event phenomena in GaAs devices and circuits," *IEEE Trans. Nucl. Sci.*, vol. 43, p. 628, 1996.

[7] P. F. Marsh, S. Kang, R. Wohlert, P. M. McIntosh, W. E. Hoke, R. A. McTaggart, S. M. Lardizabal, R. E. Leoni III, C. S. Whelan, P. J. Lemonias, and T. E. Kazior, "Millimeter-wave low noise metamorphic HEMT amplifiers and devices on GaAs substrates," in *Technical Digest 1999 GaAs Integrated Circuit Symposium*, pp. 221–223.

[8] C. S. Whelan, W. E. Hoke, R. A. McTaggart, S. M. Lardizabal, P. S. Lyman, P. F. Marsh, and T. E. Kazior, "Low noise $In_{0.32}(AlGa)_{0.68}As/In_{0.43}Ga_{0.57}As$ metamorphic HEMT on GaAs substrate with 850 mW/mm output power density," *IEEE Electron Dev. Lett.*, vol. 21, p. 5, 2000.

[9] J. B. Boos, W. Kruppa, B. R. Bennett, D. Park, S. Kirchoefer, R. Bass, and H. B. Dietrich, "AlSb/InAs HEMTs for low-voltage, high-speed applications," *IEEE Trans. Electron Dev.*, vol. 45, p. 1869, 1998.

[10] J. B. Boos, B. R. Bennett, W. Kruppa, D. Park, J. Mittereder, R. Bass, and M. E. Twigg, "Ohmic contacts in AlSb/InAs high electron mobility transistors for low-voltage operation," *J. Vac. Sci. Technol. B*, vol. 17, p. 1022, 1999.

[11] J. B. Boos, M. J. Yang, B. R. Bennett, D. Park, W. Kruppa, C. H. Yang, and R. Bass, "0.1 μm AlSb/InAs HEMTs with InAs subchannel," *Electron. Lett.*, vol. 35, p. 1525, 1998.

[12] J. S. Melinger, D. McMorrow, A. B. Campbell, S. Buchner, L. H. Tran, A. R. Knudson, and W. R. Curtice, "Pulsed laser induced single event upset and charge collection measurements as a function of optical penetration depth," *J. App. Phys.*, vol. 84, p. 690, 1998.

[13] G. Theodorou and G. Tsegas, "Theory of electronic and optical properties of bulk AlSb and InAs and InAs/AlSb superlattices," *Phys. Rev. B*, vol. 61, p. 10 782, 2000.

[14] D. E. Aspnes and A. A. Studna, "Dielectric functions and optical parameters of Si, Ge, GaP, GaAs, GaSb, InP, InAs, and InSb from 1.5 to 6.0 eV," *Phys. Rev. B*, vol. 27, p. 985, 1983.

[15] K. Strossner, S. Ves, C. K. Kim, and M. Cardona, "Dependence of the direct and indirect gap of AlSb on hydrostatic pressure," *Phys. Rev. B*, vol. 33, p. 4044, 1986.

[16] S. Zollner, C. Lin, E. Schonherr, A. Bohringer, and M. Cardona, "The dielectric function of AlSb from 1.4 to 5.8 eV determined by spectroscopic ellipsometry," *J. Appl. Phys.*, vol. 66, p. 383, 1989.

[17] D. McMorrow, J. S. Melinger, A. R. Knudson, S. Buchner, L. H. Tran, A. B. Campbell, and W. R. Curtice, "Charge-enhancement mechanisms of GaAs field-effect transistors: Experiment and simulation," *IEEE Trans. Nucl. Sci.*, vol. 45, p. 1494, 1998.

[18] T. R. Weatherford, D. McMorrow, W. R. Curtice, A. R. Knudson, and A. B. Campbell, "Single event induced charge transport modeling of GaAs MESFETs," *IEEE Trans. Nucl. Sci.*, vol. 40, p. 1867, 1993.

[19] J. R. Schwank, F. W. Sexton, T. R. Weatherford, D. McMorrow, A. R. Knudson, and J. S. Melinger, "Charge collection in GaAs MESFETs fabricated in semi-insulating substrates," *IEEE Trans. Nucl. Sci.*, vol. 42, p. 1585, 1995.

[20] B. W. Hughlock, T. Williams, A. H. Johnston, and R. E. Plaag, "Ion-induced charge collection GaAs MESFETs and its effect on SEU vulnerability," *IEEE Trans. Nucl. Sci.*, vol. 38, p. 1442, 1991.